Stabilities and Energetics of Pentacoordinated Carbonium Ions. The Isomeric $C_2H_7^+$ Ions and Some Higher Analogues: $C_3H_9^+$ and $C_4H_{11}^+$

Kenzo Hiraoka and Paul Kebarle*

Contribution from the Chemistry Department, University of Alberta, Edmonton, Alberta, Canada T6G 2E1. *Received December 5, 1975*

Abstract: The kinetics and equilibria of reaction 1 were studied in H_2 gas at 1–5 Torr over the temperature range −160 to 200 °C. The experiments were done in a pulsed electron beam high pressure ion source mass spectrometer. At the lowest temperatures (−160 to −130 °C) reaction 1 reached equilibrium. The forward rate of (1) decreased with increasing temperature. This means that the $C_2H_7^+$(a) formed at this temperature was a result of an exothermic third body dependent reaction without activation energy. Measurement of the temperature dependence of the equilibrium led to $\Delta H_{1a} = -4.0$ kcal/mol and $\Delta H_f(C_2H_7^+(a)) = 215$ kcal/mol. At temperatures above −130 °C, where $C_2H_7^+$(a) was unstable, little $C_2H_7^+$ could be observed. Between −100 and 40 °C a new species $C_2H_7^+$(b) was formed by a second-order process (reaction 1b). The rate constant k_{1b} for this reaction increased with temperature. The activation energy was $E_{1b} = 1.2$ kcal/mol. At temperatures between 40 and 200 °C, $C_2H_7^+$(b) began to decompose to $C_2H_5^+ + H_2$ and an equilibrium (reaction 1b) could be measured giving $\Delta H_{1b} = -11.8$ kcal/mol and $\Delta H_f(C_2H_7^+(b)) = 207$ kcal/mol. The C_2H_7(a) is identified with the C–H protonated ethane structure A which, however, is very close to an undisturbed ethyl ion and an H_2 molecule. The more stable structure $C_2H_7^+$(b) is identified as B, the C–C protonated structure of ethane. The energy barrier between species (a) and (b) is $E_{1b} - \Delta H_{1a} = 5.2$ kcal/mol. Earlier results on the species $C_3H_9^+$ are combined with new measurements to establish the energetics of two experimental species $C_3H_9^+$(a) which corresponds essentially to *sec*-$C_3H_7^+$ interacting very weakly with H_2 and the $C_3H_9^+$(b) species of a structure similar to B. The heats of formation are $\Delta H_f(C_3H_9^+(a)) = 189.5$ kcal/mol and $\Delta H_f(C_3H_9^+(b)) = 194.5$ kcal/mol. Thus for the propanes the (a) species has the lower heat of formation. However, the (b) species is more stable with respect to dissociation. The potential energy barrier between $C_3H_7^+$(a) and $C_3H_7^+$(b) is ~14 kcal/mol. Two analogous structures for $C_4H_{11}^+$ are also investigated. Proton affinities for protonation to the respective isomers are also derived.

The pentacoordinated methonium ion CH_5^+ was among the first ion–molecule reaction products observed with mass spectrometers.[1] The next higher analogue $C_2H_7^+$ was also observed relatively early.[2] However, until recently no clear experimental evidence for the existence and stability of higher protonated alkanes was available.

The bonding in CH_5^+ was considered in several theoretical papers[3-8] which ultimately agreed on the three center-bonded structure with C_s symmetry shown below as being the most stable. Ab initio calculations[4] (STO-3G) for the $C_2H_7^+$ ion predicted two stable isomers, the C–H protonated structure (A) and the C–C protonated structure (B) shown below. The

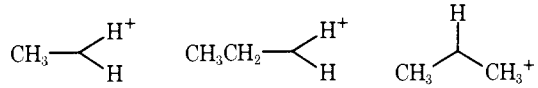

A B

structure (B) was found[4] more stable by some 10–12 kcal/mol. However, more recently results obtained with the simpler semiempirical[9] MINDO/3 predicted structure (A) to be more stable. More accurate ab initio calculations with larger basis sets and correlation interaction for the $C_2H_7^+$ species will probably be forthcoming in the near future.[10,11]

Great interest in pentacoordinated carbonium ions in solution was created by the work of Olah.[12] It was largely this work that increased the awareness that pentacoordinated carbonium ions are interesting not only from the standpoint of bonding and structural theory but also as intermediates in aliphatic substitution reactions of alkanes like acid-catalyzed fragmentation, isomerization, and cyclization.

Experimental information on the heats of formation, energetics, and reactivity of such carbonium ions, in the gas phase, is clearly of considerable interest. Recently studies of several ion–molecule equilibria involving three center-bonded carbonium ions in the gas phase were made in the present laboratory.[13-17] Guided by these results it occurred to us that a study of the temperature dependence of the rates and equilibria for reaction 1 might lead to information on the stabilities of the different $C_2H_7^+$ isomeric structures.

$$C_2H_5^+ + H_2 = C_2H_7^+ \qquad (1)$$

The existence of previous results[15,16] on the species $C_3H_9^+$ formed from $C_2H_5^+ + CH_4$ suggested some additional experiments involving $C_3H_9^+$ isomers and $C_4H_{11}^+$ isomers. The combined results of these studies lead to an interesting survey of energetics and stabilities of the lower protonated alkanes.

Experimental Section

(a) General. The measurements were made with the pulsed electron beam high pressure ion source mass spectrometer which has been described previously.[18]

The $C_2H_5^+ + H_2 = C_2H_7^+$ experiments were done with H_2 gas containing known small quantities of CH_4. The H_2 gas (Linde UHP) was further purified by passing it through a liquid nitrogen cooled trap containing molecular sieve 5 Å. Downstream of this trap CH_4 (Linde UHP) gas was added to the H_2 stream through a calibrated capillary. The H_2, CH_4 mixture was passed through another liquid N_2 cooled trap with molecular sieve 5 Å and then in and out of the ion source. Initially this trap retains CH_4; however, after some time it becomes saturated and lets this gas through. The CH_4 concentration could also be followed by observation of the $CH_5^+(CH_4)_n$ equilibria whose equilibrium constants had been determined earlier.[14] Rigorous attention to the purification procedure allowed one to eliminate all other impurities including water and C_2H_6. The absence of impurities was attested by the fact that the $CH_5^+(CH_4)_n$ ion group had stationary concentrations with time. The presence of impurities would have caused an observable decrease of these ions because of proton transfer to the impurity.

(b) The Reaction System. Production of $C_2H_5^+$ in H_2 Gas. The kinetics and equilibria of reaction 1 must be studied in hydrogen as the major gas. Various alternatives exist for the production of $C_2H_5^+$. In the present high pressure ion source apparatus[18] the production and reactions of a given ion occur in the same region, i.e., the ion source. Since, as will be seen in the next sections, at low temperatures the interaction of $C_2H_5^+$ with H_2 is quite weak, the presence of many a gas that could be used for the production of $C_2H_5^+$ is detrimental since this gas will likely react with $C_2H_5^+$. A similar difficulty is encoun-

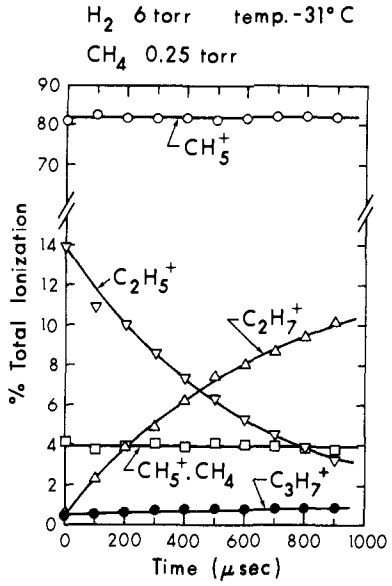

Figure 1. Concentration changes of major ions observed in 6 Torr of H_2 containing 0.25 Torr of CH_4 at −31 °C after the electron pulse. (Duration of electron pulse ~80 μs.) The decrease of $C_2H_5^+$ and the increase of $C_2H_7^+$ are attributed to reaction 1b, $C_2H_5^+ + H_2 = C_2H_7^+$(b), where $C_2H_7^+$(b) is an isomer stable at higher temperatures.

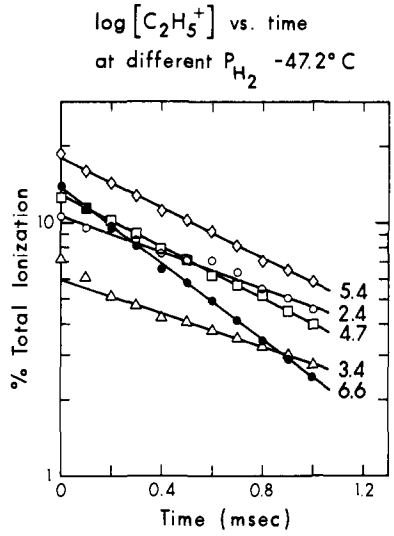

Figure 2. Logarithmic plot of the decay of $C_2H_5^+$ with time because of reaction 1b. Runs at constant temperature −47.2 °C but different H_2 pressures. Slope ν_{1b} of plots increases with increasing H_2 pressure. Numbers beside curves indicate H_2 pressure in Torr.

tered also at higher temperatures since the reaction 1b (see Results and Discussion) proceeds with a very low rate constant. Because of the above difficulties the gas mixture selected was H_2 gas at pressures 2–7 Torr containing small quantities of methane (200–0.4 mTorr).

Electron impact with the major gas leads[20] mainly to H_2^+ by (2). Only about 1–2% of H^+ is produced by (3). Electron impact with the minor gas leads[20] mainly to CH_4^+ and CH_3^+ roughly in 1:1 ratio.

$$H_2 + e = H_2^+ + 2e \quad (2)$$

$$H_2 + e = H^+ + H + 2e \quad (3)$$

The major ion-molecule reaction is (6) followed by proton transfer to methane (reaction 7) which creates the major ion CH_5^+.

$$e + CH_4 = CH_4^+ + 2e \quad (4)$$

$$e + CH_4 = CH_3^+ + H + 2e \quad (5)$$

$$H_2^+ + H_2 = H_3^+ + H \quad (6)$$

$$H_3^+ + CH_4 = CH_5^+ + H_2 \quad (7)$$

Since the concentration of CH_4 is very much smaller than that of H_2 only a small fraction of H_2^+ reacts with CH_4. The major product of this reaction[21] is CH_3^+ by (8).

$$H_2^+ + CH_4 = CH_3^+ + H + H_2 \quad (8)$$

Since the third body dependent conversion of H^+ to H_3^+ by reaction 9 is quite slow ($k_9 \approx 10^{-29}$ cm^6 molecules^{-2} s^{-1})[19] even at low concentrations of CH_4 some CH_3^+ might be produced by reaction 10.

$$H^+ + 2H_2 = H_3^+ + H_2 \quad (9)$$

$$H^+ + CH_4 = CH_3^+ + H_2 \quad (10)$$

The CH_3^+ created by (5), (8), and (10) reacts with CH_4 to give $C_2H_5^+$ by the well-known reaction 11. It is this reaction which is the source of the $C_2H_5^+$ ions used in the present study.

$$CH_3^+ + CH_4 = C_2H_5^+ + H_2 \quad (11)$$

The ions observed in a typical run are shown in Figure 1. The ions CH_5^+ and $CH_5^+(CH_4)$ represent some 86% of the total ions. The $CH_5^+(CH_4)_n$ ions result from clustering reactions like (12) which were studied earlier.[14]

$$CH_5^+ + CH_4 + M = CH_5^+(CH_4) + M \quad (12)$$

As noted from Figure 1, the $CH_5^+(CH_4)_n$ group of ions remains a constant proportion of the total ions, i.e., these ions do not react further. The initial concentration of $C_2H_5^+$, the only other initial ion observed, is ~14%. Reactions 1 to 11 are very rapid in the present system and are complete at the end of the ionizing pulse. The pressure ratio H_2:CH_4 for the run (Figure 1) is 24. The ionization cross sections σ for processes 2 + 3 and 4 + 5 are approximately[22] $\sigma(2+3)/\sigma(4+5) \approx 1/4$. The rate constant ratio[21] $k_6/k_8 \approx 0.6$. A consideration of these figures leads one to expect that the initial $C_2H_5^+$ should be approximately 11%. The observed somewhat higher 14% concentration might be due to the contribution of reaction 10 to the production of CH_3^+.

Results and Discussion

(a) Kinetics of Reaction 1b in the High-Temperature Range (−100 to 40 °C). The results from a typical run obtained at −31 °C with hydrogen containing traces of methane were presented in Figure 1. The reactions involved in the rapid production of $C_2H_5^+$ in this system were discussed in the Experimental Section. The ions $CH_5^+(CH_4)_n$, which are also produced, are unreactive in the given gas mixture and their combined concentration does not change with time.

The $C_2H_5^+$ ion is observed to decrease with time (Figure 1). The decrease is almost completely accounted for by the increase of $C_2H_7^+$. This reactive change is attributed to reaction 1b.

$$C_2H_5^+ + H_2 = C_2H_7^+(b) \quad (1b)$$

The $C_2H_7^+$ formed in this high-temperature range is called $C_2H_7^+$(b) since, as will be seen later, a $C_2H_7^+$(a) with different properties is observed at lower temperatures.

A small increase is observed also for the ion $C_3H_7^+$. This ion should be resulting from the slow reaction 13 which was reported earlier.[16]

$$C_2H_5^+ + CH_4 = C_3H_7^+ + H_2 \quad (13)$$

Using values for k_{13} from that earlier work,[16] one calculates $C_3H_7^+$ yields in approximate agreement with those observed in the present experiments. In all runs concentration conditions were so selected as to lead to $C_3H_7^+$ production which was only a small fraction of the $C_2H_7^+$ yield. This allowed one to neglect reaction 13 as a cause of $C_2H_5^+$ decrease.

The decrease of $C_2H_5^+$ and the corresponding increase of $C_2H_7^+$(b) was measured in a series of runs in the temperature range −100 to 40 °C. The dependence of reaction 1b on the pressure of the major gas H_2 was also examined in several runs, where the pressure of H_2 was increased at constant tempera-

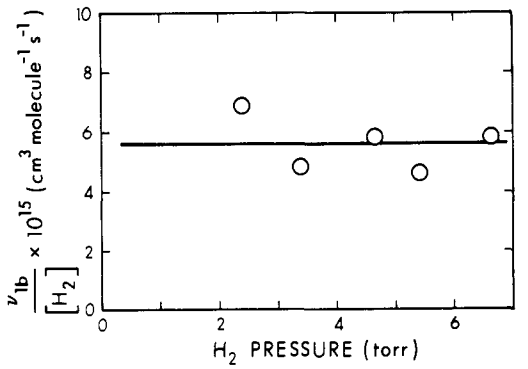

Figure 3. Plot of slope $\nu_{1b}/[H_2]$ from Figure 2 vs. pressure of H_2 used. Result shows that rate constant k_{1b} is first order in H_2 concentration, thus overall second order.

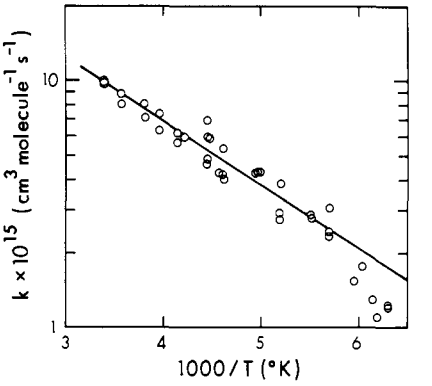

Figure 4. Arrhenius plot of temperature-dependent rate constants k_{1b} for the reaction $C_2H_5^+ + H_2 = C_2H_7^+$(b). Straight line obtained leads to $k_{1b} = 7.3 \times 10^{-14} \exp(-1.2 \text{ kcal}/RT)$ molecules^{-1} cm^{-3} s^{-1}.

ture. Results from one series of such experiments are shown in Figure 2. Plots of log $[C_2H_5^+]$ vs. time give straight lines. The slopes ν_{1b} of the lines increase with H_2 pressure. The slopes ν_{1b} divided by $[H_2]$ are given in Figure 3. The plot indicates that $\nu_{1b}/[H_2] = k_{1b}$ is independent of $[H_2]$. This means that reaction 1b is first order in $[C_2H_5^+]$ and first order in $[H_2]$, i.e., overall second order.

Determinations of k_{1b} based on the decay of $[C_2H_5^+]$ at different temperatures were used to construct the Arrhenius plot shown in Figure 4. The straight line obtained defines the relationship

$$k_{1b} = (7.3 \pm 0.9) \times 10^{-14} \exp\left(\frac{-1.2 \pm 0.1 \text{ kcal/mol}}{RT}\right) \text{ molecules}^{-1} \text{ cm}^3 \text{ s}^{-1} \quad (14)$$

The temperature range covered by the plot (Figure 4) was limited between −100 and 40 °C since at lower temperatures the reaction became too slow while at higher temperatures the reverse decomposition of $C_2H_7^+$ to $C_2H_5^+ + H_2$ began to interfere.

Reaction 1b is an exothermic association process and at first glance not a second-order but a third-order rate dependence might have been expected at the relatively low pressures of the experiments. Third-order dependence has been found for a large number of exothermic ion–molecule association reactions.[23] However, there is one characteristic difference. The third-order reactions have no activation energy barrier for the formation of the ion–molecule adduct. In fact, because of temperature-dependent decrease of the lifetime of the internally excited adduct these reactions have negative temperature coefficients.[23] In the present case there is a *positive* temperature dependence. The observed second-order dependence for the present case must come about because a small fraction of reactants (those on the high energy end of the Maxwell distribution) pass the activation barrier to form the adduct. Thus while the adduct will contain excess energy, this excess energy will be nearly equal to the potentail energy difference between the zero-point energy of the adduct and the top of the energy barrier for back dissociation to the reactants. This means that the adduct will be relatively long lived and efficiently stabilized by third-body collisions. The situation in exothermic adducts formed without barrier is different since in that case all reactant molecules, and not only the high energy Maxwell tail, participate in the formation of the adduct. The adduct thus contains excess (thermal) energy and is shorter lived, i.e., the rate of formation remains third-body dependent up to higher pressures.

(b) Equilibria of Reaction 1b in the High-Temperature Range 85–200 °C. As mentioned in the previous section the reverse of reaction 1b begins to interfere with the determination of the forward rate at temperatures above 40 °C.

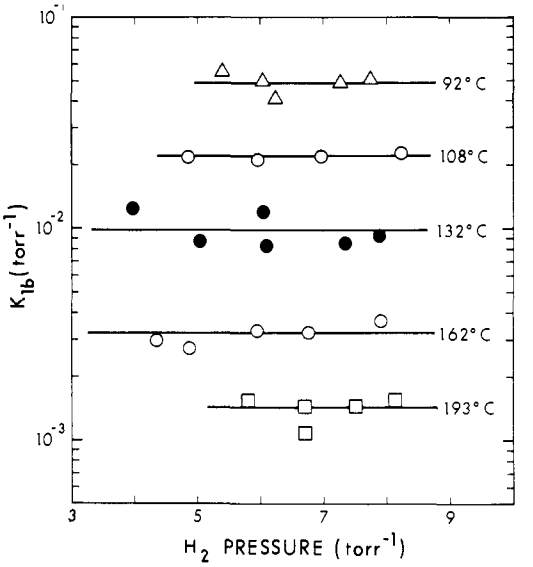

Figure 5. Values of equilibrium constants K_{1b} for reaction $C_2H_5^+ + H_2 = C_2H_7^+$(b) which reaches equilibrium between 80 and 200 °C. Values are independent of hydrogen pressure.

$$C_2H_5^+ + H_2 = C_2H_7^+(b) \quad (1b)$$

The forward and reverse rates become comparable above 85 °C and it becomes possible to measure the equilibrium constant K_{1b} in the temperature range 85–200 °C. By measuring the time-independent concentrations of $C_2H_5^+$ and $C_2H_7^+$ it was possible to show that K_{1b} is independent of H_2 pressure. Such variable pressure results at a constant reaction temperature are shown in Figure 5.

A van't Hoff plot of the equilibrium constants is shown in Figure 6. The slope of the straight line leads to $\Delta H_{1b} = -11.8 \pm 0.4$ kcal/mol and $\Delta S°_{1b} = -25 \pm 1$ eu (standard state 1 atm). The lowest temperature point in Figure 6 was not obtained by direct equilibrium measurement but from the ratio $K = k_f/k_r$ where $k_f = k_{1b}$ is a rate constant determined in the previous section and $k_r = k_{-1b}$ is a value from a pyrolysis study of $C_2H_7^+$ done previously in this laboratory.[17] As can be seen this experimental point which is in the experimental range of the two independent rate constant determinations is in agreement with the present high-temperature equilibrium measurements.

(c) $C_2H_5^+ + H_2 = C_2H_7^+$(a) Equilibrium at Low Temperature (−130 to −160 °C). As mentioned in section (a) the production of $C_2H_7^+$ by reaction 1b slows down as the tempera-

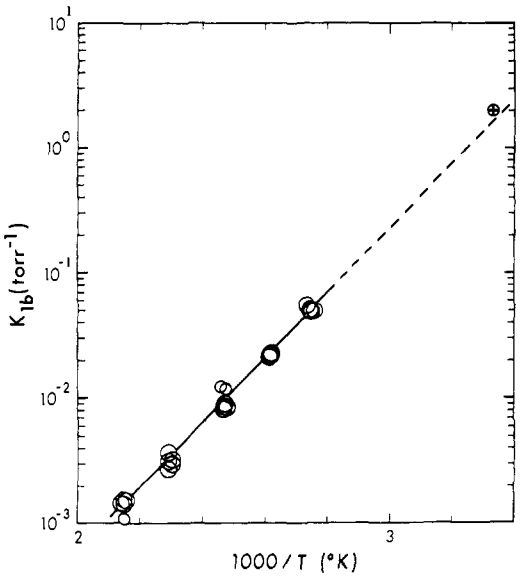

Figure 6. van't Hoff plot of equilibrium constant K_{1b}. Straight line leads to $\Delta H_{1b} = -11.8$ kcal/mol and $\Delta S_{1b} = -25$ eu (standard state 1 atm): (○) experimental points obtained in equilibrium region; (⊕) single point based on $K_{1b} = k_f/k_r$ where $k_f = k_{1b}$ obtained from the kinetic determinations in section a and k_r is a rate constant obtained in an earlier study[17] of the thermal decomposition of $C_2H_7^+$ to $C_2H_5^+ + H_2$.

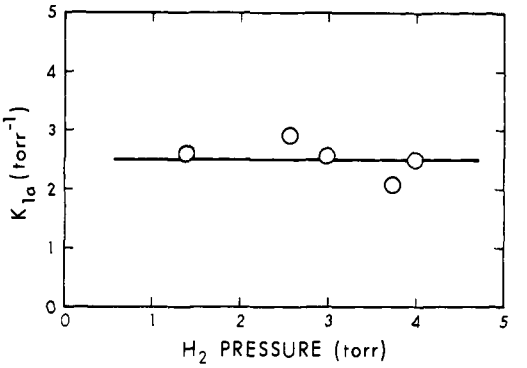

Figure 7. Pressure dependence of the equilibrium constant K_{1a} for reaction 1a, $C_2H_5^+ + H_2 = C_2H_7^+$(a), occurring at low temperatures. Data for the plot were obtained at −156 °C.

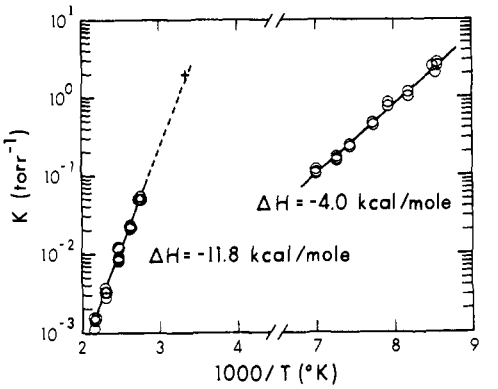

Figure 8. van't Hoff plot of equilibrium constant K_{1a} for equilibrium $C_2H_5^+ + H_2 = C_2H_7^+$(a) occurring at low temperature. Plot leads to $\Delta H_{1a} = -4.0$ kcal/mol and $\Delta S_{1a} = -19.6$ eu (standard state 1 atm). For comparison the high-temperature plot of K_{1b} leading to the high-temperature species $C_2H_7^+$(b) is also given.

ture is decreased. Below −100 °C the production rate becomes too slow to measure with the present technique. However, when the temperature was lowered some more to −130 °C and beyond, formation of $C_2H_7^+$ could be observed again. This newly born $C_2H_7^+$(a) was found to establish equilibrium with $C_2H_5^+ + H_2$ (at −130 °C) some 300 μs after the electron pulse. At lower temperature the establishment of equilibrium became *faster*. This meant that the new reaction forming $C_2H_7^+$ at *low* temperature had a *negative* temperature coefficient, a situation which would be expected for an exothermic association reaction in which the adduct forms without the system passing through an activation energy barrier. As discussed in section (a) such reactions are generally third-body dependent, i.e., third order in the pressure range used, and have negative temperature coefficients. The pressure dependence and thus the kinetic order of the low-temperature reaction could not be established because of interference by the previously studied[15] clustering reaction 15 whose occurrence was signalled by the appearance of the $C_3H_9^+$ ion at low temperature.

$$C_2H_5^+ + CH_4 = C_3H_9^+ \qquad (15)$$

The equilibrium 1a could be measured over the temperature range −130 to −160 °C.

$$C_2H_5^+ + H_2 + H_2 = C_2H_7^+(a) + H_2 \qquad (1a)$$

Because of the interference of reaction 15 these runs were made with very low CH_4 concentration ($P_{CH_4} \approx 2 \times 10^{-4}$ Torr). This reduced very much the creation rate of $C_2H_5^+$ ions (see the Experimental Section) such that the $C_2H_5^+$ and $C_2H_7^+$ ions represented less than 1% of the total ions, all other ions being $CH_5(CH_4)_n^+$ species. Unfortunately this made the equilibria measurements somewhat difficult. An examination of the independence of the equilibrium constant of the H_2 pressure was made at only one temperature. These results are displayed in Figure 7. A van't Hoff plot of the equilibrium constants obtained at different temperatures is shown in Figure 8. The slope leads to $\Delta H_{1a} = -4.0 \pm 0.5$ kcal/mol while the entropy change is $\Delta S°_{1a} = -19.6 \pm 1.5$ eu. The extrapolated free energy change to room temperature (300 K) is $\Delta G°_{1a} = +1.8$ kcal/mol (standard state 1 atm). Evidently the $C_2H_7^+$(a) is unstable with respect to dissociation to $C_2H_5^+ + H_2$ even at 1 atm of hydrogen gas at 300 K.

The data obtained in sections (a)–(c) will be used in the next section to determine the enthalpies of formation of $C_2H_7^+$(a) and $C_2H_7^+$(b) and correlate these species with the $C_2H_7^+$ isomers.

(d) Thermochemical Data and Identity of $C_2H_7^+$(a) and $C_2H_7^+$(b). The $\Delta H_{1b} = -11.8$ kcal/mol for the formation of the "high"-temperature $C_2H_7^+$(b) species from $C_2H_5^+$ and H_2 when combined with the known[24] $\Delta H_f(C_2H_5^+) = 219$ kcal/mol leads to $\Delta H_f(C_2H_7^+(b)) = 207.2$ kcal/mol and to a proton affinity of ethane $PA(C_2H_6) = 139.6$ kcal/mol for protonation leading to $C_2H_7^+$(b). Similarly the $\Delta H_{1a} = -4.0$ kcal/mol for the low-temperature species $C_2H_7^+$(a) leads to $\Delta H_f(C_2H_7^+(a)) = 215$ kcal/mol and $PA(C_2H_6) = 131.8$ kcal/mol (a). These data are summarized in Table I.

Also included in Table I, for comparison purposes, are $\Delta H_f(CH_5^+)$ and $PA(CH_4)$ obtained from literature data.[25,26]

The more stable $C_2H_7^+$(b) has been observed before. As mentioned earlier, a study of the pyrolysis of $C_2H_7^+$ to $C_2H_5^+ + H_2$ in this laboratory[17] led to an activation energy $E = 10.5 \pm 2$ kcal/mol. Since $\Delta H_{1b} \approx E_{1b} - E_{-1b}$, where (−1b) refers to the reverse of (1b), and $E_{1b} = 1.2$ kcal/mol (see eq 14), one expects that $E_{-1b} = 11.8 + 1.2 = 13$ kcal/mol. The earlier observed[17] $E = 10.5 \pm 2$ kcal/mol is lower than that value but still within the expected error limits of the measurements. We conclude that the $C_2H_7^+$ of the pyrolysis study[17] was $C_2H_7^+$(b). This species was prepared[17] by reaction 16 at temperatures up to 230 °C.

$$CH_5^+ + C_2H_6 = CH_4 + C_2H_7^+(b) \qquad (16)$$

Table I. Thermochemical Data for Protonated Alkanes[a]

Reaction	ΔH	ΔH_f(alkane H^+)[b]	Barrier a → b	PA(alkane)[c]
$CH_5^+ = CH_3^+ + H_2$	40	221.1[d]		127[d]
$C_2H_7^+(a) = C_2H_5^+ + H_2$	4.0	215	5.2	131.8
$C_2H_7^+(b) = C_2H_5^+ + H_2$	11.8	207.2		139.6, 140.4[f]
$C_3H_9^+(a) = sec\text{-}C_3H_7^+ + H_2$	≤2.5	≥189.5	≤14.0[e]	≤152.8
$C_3H_9^+(b) = C_2H_5^+ + CH_4$	6.6[e]	194.5		147.8
$C_4H_{11}^+(a) = t\text{-}C_4H_9^+ + H_2$	~1	168	>2.7	166.8
$C_4H_{11}^+(b) = sec\text{-}C_3H_7^+ + CH_4$	3.4	170.7		164.0

[a] All values in kcal/mol. Protonated alkanes (a) and (b) indentified in Figure 10 as corresponding A and B structures. [b] Heats of formation of all protonated alkanes except CH_5^+ based on experimentally measured ΔH reaction and ΔH_f(alkyl ion). Values of Lossing and Semeluk[24] (and W. Tsang, *J. Phys. Chem.*, **76**, 143 (1972)) were used: $\Delta H_f(C_2H_5^+) = 219$, $\Delta H_f(sec\text{-}C_3H_7^+) = 192$, and $\Delta H_f(t\text{-}C_4H_9^+) = 169$. [c] All proton affinities except that of CH_4 were evaluated from ΔH_f of the corresponding protonated alkane and $\Delta H_f(H^+) = 367$ kcal/mol. [d] Thermochemical data for CH_4 and CH_5^+ based on literature values in ref 25 and 26. [e] See also ref 15 and 16. [f] Reference 26.

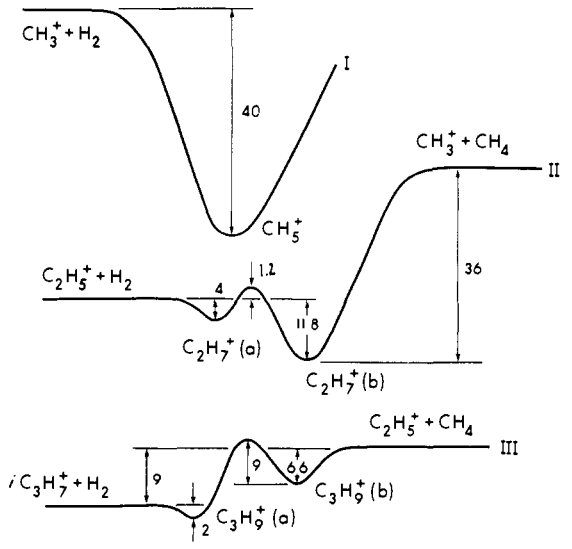

Figure 9. Schematic potential energy diagrams for some isomeric protonated lower alkanes. Diagram I is based on literature data for CH_5^+. Diagram II is based on reactions $C_2H_5^+ + H_2 = C_2H_7^+(a)$ (1a), $\Delta H_{1a} = -4.0$ kcal/mol, occurring at low temperature; and $C_2H_5^+ + H_2 = (C_2H_7^+(a)) = C_2H_7^+(b)$ (1b) occurring at higher temperature. Activation energy $E_{1b} = 1.2$ kcal/mol and $\Delta H_{1b} = -11.8$ kcal/mol. Species $C_2H_7^+(a)$ and $C_2H_7^+(b)$ are identified in the text as having structures A and B shown in Figure 10. Diagram III is for $C_3H_9^+$ based on earlier work[15,16] (see text) and $\Delta H < -2.5$ kcal/mol for reaction $sec\text{-}C_3H_7^+ + H_2 = C_3H_9^+(a)$.

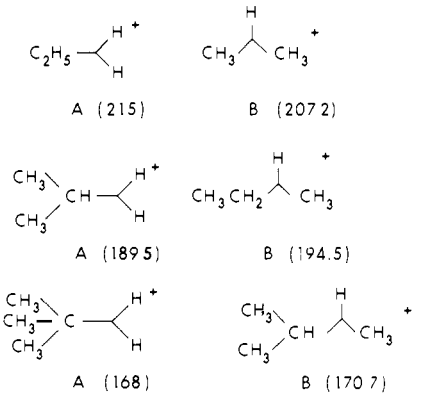

Figure 10. Structures and heats of formation for some protonated lower alkanes. Structures A and B identified in the text as experimentally observed structures a and b (see also Figure 9). Structure A is very unstable for dissociation to ion + H_2.

Reaction 16 is exothermic by some 12 kcal/mol (see Table I). This makes it very likely that $C_2H_7^+(b)$ is the most stable structure of $C_2H_7^+$, since the exothermicity of reaction 16 and the thermal energy of the reactants at 230 °C should be sufficient to overcome a possible energy barrier for the path leading to the most stable structure. The proton affinity $PA(C_2H_6) = 139.6$ kcal/mol based on ΔH_{1b} is very close to $PA(C_2H_6) = 140.4$ kcal/mol which can be deduced from Bohme's[26] proton equilibria measurements. The proton transfer process used by Bohme was reaction 17, undertaken at room temperature. As expected, the $C_2H_7^+$ formed at room temperature by (17) is identical with the $C_2H_7^+(b)$.

$$HCO^+ + C_2H_6 = CO + C_2H_7^+ \qquad (17)$$

The low-temperature, less stable $C_2H_7^+(a)$ is formed from $C_2H_5^+$ and H_2 without activation energy. (See section c.) Since the $\Delta H_{1a} = -4.0$ kcal/mol is quite low, it is natural to assume that the $C_2H_7^+(a)$ consist essentially of a $C_2H_5^+$ ion weakly interacting with the electron pair bond of a H_2 molecule. The formation of such a structure, by the electrophilic attack of $C_2H_5^+$ on H_2, can be expected to occur without activation energy. Further, it is to be expected that reaction 1b proceeds via the intermediate $C_2H_7^+(a)$. This means reaction 1b should be written as shown below.

$$C_2H_5^+ + H_2 = (C_2H_7^+(a))^* = C_2H_7^+(b) \qquad (1b)$$

A summary of the above considerations is given in the schematic potential energy diagram for experimentally observed isomeric $C_2H_7^+$ ions given in Figure 9(II). The first potential minimum, corresponding to the formation of $C_2H_7^+(a)$ from $C_2H_5^+$ and H_2, is obtained from $\Delta H_{1a} = -4.0$ kcal/mol. The barrier between $C_2H_7^+(a)$ and $C_2H_7^+(b)$ corresponds to $-\Delta H_{1a} + E\text{linfc1b} = 5.2$ kcal/mol. The depth of the minimum representing $C_2H_7^+(b)$ was obtained from $\Delta H_f(C_2H_7^+(b))$ and the known[24] heats of formation of CH_4 and CH_3^+.

We consider it most likely that the more stable $C_2H_7^+(b)$ corresponds to the C–C protonated ethane structure $C_2H_7^+$ B shown in Figure 10. The 5.2 kcal/mol barrier between $C_2H_7^+(a)$ and $C_2H_7^+(b)$ is then a consequence of the considerable structural change occurring between the $C_2H_7^+(a)$ which is a loose $C_2H_5^+ \cdot H_2$ complex and the $C_2H_7^+(b)$ whose structure is B.

It could be argued that the experimental results also fit an alternate interpretation where $C_2H_7^+(a)$ is still the $C_2H_5^+ \cdot H_2$ loose complex but the $C_2H_7^+(b)$ is a tight $C_2H_5^+ \cdot H_2$ complex, i.e., the "true" three-center bonded structure A (Figure 10). This interpretation faces the difficulty of explaining the experimentally observed barrier between $C_2H_7^+(a)$ and $C_2H_7^+(b)$. Also this interpretation would imply that structure B has such properties that its presence could not be detected by the experiments so far performed, including the proton transfer reactions 16 and 17. One comes to the paradoxical

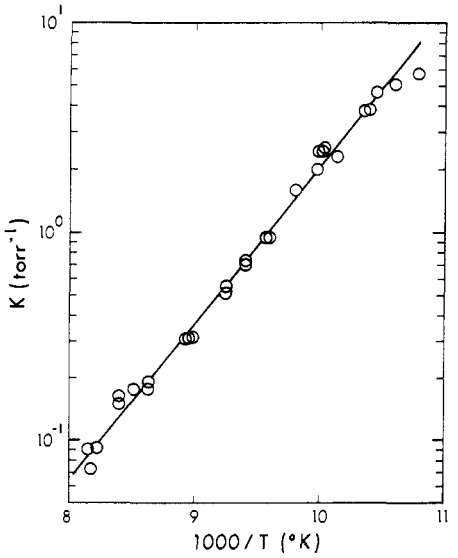

Figure 11. van't Hoff plot for equilibrium constants K_{18} for reaction *sec*-$C_3H_7^+ + CH_4 = C_4H_{11}^+$(b). Straight line gives $\Delta H°_{18} = -3.4$ kcal/mol and $\Delta S°_{18} = -20$ eu (standard state 1 atm).

requirement that the differences between the weakly and strongly bonded $C_2H_7^+$ A should be experimentally more noticeable than the differences between A and B.

We conclude that the $C_2H_7^+$(a) must correspond to the only stable $C_2H_7^+$ A structure and happens to be a very weakly bonded $C_2H_5^+ \cdot H_2$ complex. A structure in which the $C_2H_5^+$ and H_2 are closer to each other is assumed to be of higher energy and not lying in a potential minimum.

The diagram I for the CH_5^+ ion is also given in Figure 9 for comparison. It is based on the data in Table I. The ab initio calculation by Kutzelnigg[8] for the potential energy of $CH_3^+ + H_2$ approaching along a minimum energy reaction path to form CH_5^+ shows a monotonous decrease of energy.[8] We have incorporated this plausible result into diagram I. The same assumption was made also in diagram II for the approach of $C_2H_5^+$ to H_2.

The potential energy diagram III of Figure 9 is discussed in the next section.

(e) The Equilibria *sec*-$C_3H_7^+ + CH_4 = C_4H_{11}^+$ and *sec*-$C_3H_7^+ + H_2 = C_3H_9^+$ and Thermochemistry of Protonated Propanes and Isobutanes. Equilibrium 18 could be easily measured in 1–3 Torr of pure methane at low temperatures.

$$sec\text{-}C_3H_7^+ + CH_4 = C_4H_{11}(b) \qquad (18)$$

The *sec*-$C_3H_7^+$ is formed by reaction 13 (see section (a)). A van't Hoff plot of K_{18} is shown in Figure 11. The plot leads to $\Delta H°_{18} = -3.4$ kcal/mol and $\Delta S°_{18} = -20$ eu (standard state 1 atm).

Attempts were also made to measure equilibrium 19

$$sec\text{-}C_3H_7^+ + H_2 = C_3H_9^+(a) \qquad (19)$$

A mixture consisting of 3–5 Torr of H_2 containing traces of isobutane (less than 0.1 mTorr) produced abundant $C_3H_7^+$ ions at low temperatures. The *sec*-$C_3H_7^+$ ions probably resulted from the dissociative proton transfer reaction 20. The removal of $C_3H_7^+$ by the hydride transfer reaction 21 was relatively slow and caused only a gradual decrease of the $C_3H_7^+$ ion.

$$H_3^+ + i\text{-}C_4H_{10} = H_2 + sec\text{-}C_3H_7^+ + CH_4 \qquad (20)$$

$$C_3H_7^+ + i\text{-}C_4H_{10} = C_3H_8 + t\text{-}C_4H_9^+ \qquad (21)$$

No formation of $C_3H_9^+$ ions could be observed in the temperature range −130 to −170 °C. From the failure to observe these ions we conclude that the binding energy of H_2 to *sec*-$C_3H_7^+$ is very low. Since a concentration of $C_3H_9^+$ greater than 10% of the $C_3H_7^+$ concentration would have been easily detected even at the longest reaction time (2 ms) one can set an upper limit for the equilibrium concentration ratio $[C_3H_9^+]/[C_3H_7^+] < 0.1$. For a temperature of −170 °C, $p(H_2) = 3$ Torr and an assumed $\Delta S°_{19} = -20$ eu; this leads to a $-\Delta H°_{19} \leq 2.5$ kcal/mol.

The result for ΔH_{19} combined with the known[24] heat of formation of *sec*-$C_3H_7^+$ leads to $\Delta H_f(C_3H_9^+(a)) \geq 189.5$ kcal/mol given in Table I. The extremely low dissociation energy to *sec*-$C_3H_7^+$ and H_2 indicates that the $C_3H_9^+$(a) is essentially a *sec*-$C_3H_7^+$ ion weakly interacting with an H_2 molecule. In an earlier study[15,16] of protonated propanes we measured the enthalpy change for reaction 15. The value $\Delta H_{15} = -6.6$ kcal/mol was obtained.

$$C_2H_5^+ + CH_4 = C_3H_9^+(b) \qquad (15)$$

This leads to $\Delta H_f(C_3H_9^+(b)) = 194.5$ kcal/mol. We reasoned that $C_3H_9^+$(b) had the C–C protonated three-center bonded structure B shown in Figure 10 since it was formed without activation energy by the electrophilic attack of the ethyl ion on a C–H bond in methane. The very loosely bonded *sec*-$C_3H_7^+ \cdot H_2 = C_3H_9^+$(a) can be formally assigned the C–H protonated structure A (Figure 10).

In earlier work[16] it was also observed that at higher temperatures the reaction of $C_2H_5^+ + CH_4$ did not lead to $C_3H_9^+$(b) but proceeded as in (13). An activation energy $E_{13} = 2.5$ kcal/mol was determined.

$$C_2H_5^+ + CH_4 = [C_3H_9^+(b)] \rightarrow sec\text{-}C_3H_7^+ + H_2 \qquad (13)$$

The experimental data for the $C_3H_9^+$ species are summarized in Table I and in the schematic potential energy diagram III in Figure 9. The potential barrier between $C_3H_9^+$(a) and $C_3H_9^+$(b) of ≤14.0 kcal/mol was obtained by adding $E_{13} = 2.5$ kcal/mol to the difference: $\Delta H_f(C_2H_5^+) + \Delta H_f(CH_4) - \Delta H_f(C_3H_9^+(a)) \leq 11.5$ kcal/mol.

In the earlier work[16] we had identified the C–H protonated structure A with the top of the 12.5 kcal/mol barrier. This structure A was meant to be a "true" three-center bonded species in which the H_2 is brought close to the positive center of the isopropyl ion in spite of the resulting increase of energy. In Figure 9 we have identified structure A with $C_3H_9^+$(a), i.e., with the potential minimum of the *sec*-$C_3H_7^+ \cdot H_2$ system since the resulting complex even though extremely weakly bonded can still formally be considered as a C–H protonated structure A.

It is interesting to note that the heat of formation of structure $C_3H_9^+$(a) is lower than that of structure (b). The opposite was true for the ethanes. The low heat of formation of the $C_3H_9^+$(a) is due to the stabilization of the isopropyl ion by the two methyl groups. The stabilization is so efficient that essentially no energy can be gained by an electrophilic attack on the tight H–H bond. Thus the $C_3H_9^+$(a) has the lower heat of formation but it is a "nonspecies" since it can exist only at lowest temperatures. On the other hand $C_3H_9^+$(b) is much more stable toward dissociation to $C_2H_5^+ + CH_4$ (6.6 kcal/mol) or *sec*-$C_3H_7^+ + H_2$ (9 kcal/mol).

The enthalpy for reaction 18, $\Delta H_{18} = -3.4$ kcal/mol, in which $C_4H_{11}^+$(b) is formed from the attack of the isopropyl cation on the C–H bond in methane leads to $\Delta H_f(C_4H_{11}^+(b)) = 170.7$ kcal/mol. In analogy to the previous considerations this species should have the structure B shown in Figure 10. Since *sec*-$C_3H_7^+ \cdot H_2 = C_3H_9^+$(a) was found to require at most 2.5 kcal/mol for the dissociation to *sec*-$C_3H_7^+ + H_2$ we assume that *t*-$C_4H_9^+ + H_2 = C_4H_{11}^+$(a) should be even more weakly bonded. Assuming $\Delta H \approx 1$ kcal/mol for the dissociation to *t*-$C_4H_9^+ + H_2$ one obtains $\Delta H_f(C_4H_{11}^+(a)) \simeq 168$ kcal/mol. The values are summarized in Table I. Again the

species $C_4H_{11}^+$(a) has the lower heat of formation but is not a "real" species while $C_4H_{11}^+$(b) of structure B is more stable toward dissociation. The barrier toward CH_4 + *sec*-$C_3H_7^+$ is 3.4 kcal/mol while the barrier toward *t*-$C_4H_9^+$ + H_2 should be somewhat higher.

The proton affinities for propane and isobutane calculated from the enthalpies of formation of the respective protonated a and b species are shown in Table I. Evidently protonation would lead mostly to protolysis into an alkyl ion and CH_4 or H_2. However, at low temperatures the species b should be observable provided that the protonating agent has a proton affinity which is higher than the proton affinity relating to the b species but not by more than 1-2 kcal/mol.

Ausloos,[27] Aquilanti,[28] and Harrison[29] have studied the protolysis of labeled propane and isobutane. This work has shown that the proton transferred by the acid (H_3^+ and CH_5^+) after protolysis appears in the neutral product. For example, in the protonation of propane the proton appears in the hydrogen when the products are $C_3H_7^+$ + H_2 and in the methane when the products are $C_2H_5^+$ + CH_4. It should be noted that this result is consistent with the assumption that protolysis proceeds via the three-center bonded structures A and B, since $C_3H_9^+$ A is essentially *sec*-$C_3H_7^+ \cdot H_2$ and $C_3H_9^+$ B is close to $C_2H_5^+ \cdot CH_4$. Both structures dissociate very easily after protonation of the C-H or the C-C bond so that little time is left for proton scrambling.

References and Notes

(1) V. L. Talroze and A. L. Lyubimova, *Dokl. Akad Nauk SSSR*, **86**, 509 (1952).
(2) S. Wexler and N. Jesse, *J. Am. Chem. Soc.*, **84**, 3425 (1962); A. Henglein and G. A. Muccini, *Z. Naturforsch.*, **17**, 452 (1962). F. H. Field, J. L. Franklin, and M. S. B. Munson, *J. Am. Chem. Soc.*, **85**, 3575 (1963); P. Kebarle and E. W. Godbole, *J. Chem. Phys.*, **39**, 1131 (1963); M. S. B. Munson and F. H. Field, *J. Am. Chem. Soc.*, **87**, 3294 (1965).
(3) A. Gamba, G. Morin, and M. Simonetta, *Chem. Phys. Lett.*, **3**, 20 (1969).
(4) W. A. Lathan, W. J. Hehre, and J. A. Pople, *J. Am. Chem. Soc.*, **93**, 808 (1971).
(5) P. C. Hariharan, W. A. Lathan, and J. A. Pople, *Chem. Phys. Lett.*, **14**, 385 (1972).
(6) V. Dycymons, V. Staemler, and W. Kutzelnigg, *Chem. Phys. Lett.*, **5**, 361 (1970).
(7) W. A. Lathan, W. J. Hehre, and J. A. Pople, *Tetrahedron Lett.*, **31**, 2699 (1970).
(8) V. Dycymons and W. Kutzelnigg, *Theor. Chem. Acta*, **33**, 239 (1974).
(9) P. K. Bischof and M. J. S. Dewar, *J. Am. Chem. Soc.*, **97**, 2278 (1975).
(10) S. Huzinaga, private communication.
(11) J. A. Pople, private communication.
(12) G. A. Olah, G. Klopman, and R. H. Schlossberg, *J. Am. Chem. Soc.*, **91**, 3261 (1969); G. A. Olah, "Carbocations and Electrophilic Reactions", Wiley, New York, N.Y., 1974.
(13) K. Hiraoka and P. Kebarle, *J. Chem. Phys.*, **62**, 2267 (1975).
(14) K. Hiraoka and P. Kebarle, *J. Am. Chem. Soc.*, **97**, 4179 (1975).
(15) K. Hiraoka and P. Kebarle, *Can. J. Chem.*, **53**, 970 (1975).
(16) K. Hiraoka and P. Kebarle, *J. Chem. Phys.*, **63**, 394, 1689 (1975).
(17) M. French and P. Kebarle, *Can. J. Chem.*, **53**, 2268 (1975).
(18) A. J. Cunningham, J. D. Payzant, and P. Kebarle, *J. Am. Chem. Soc.*, **94**, 7627 (1972).
(19) T. M. Miller, J. T. Moseley, D. W. Martin, and E. W. McDaniel, *Phys. Rev.*, **173**, 115 (1968).
(20) Index of Mass Spectral Data, American Society for Testing and Materials, Philadelphia, Pa., 1963.
(21) J. K. Kim and W. T. Huntress, *J. Chem. Phys.*, **62**, 2820 (1975).
(22) J. W. Otvos and D. P. Stevenson, *J. Am. Chem. Soc.*, **78**, 5461 (1956); F. W. Lampe, J. L. Franklin, and F. H. Field, *ibid.*, **79**, 6129 (1957).
(23) J. D. Payzant, A. J. Cunningham, and P. Kebarle, *Can. J. Chem.*, **50**, 2230 (1972). E. E. Ferguson, "Ion Molecule Reactions", J. L. Franklin, Ed., Plenum Press, New York, N.Y., 1972.
(24) F. P. Lossing and G. P. Semeluk, *Can. J. Chem.*, **48**, 955 (1970).
(25) W. A. Chupka and J. Berkowitz, *J. Chem. Phys.*, **54**, 4256 (1971).
(26) D. K. Bohme, "Interactions between Ions and Molecules", P. Ausloos, Ed., Plenum Press, New York, N.Y., 1975.
(27) P. Ausloos, S. G. Lias, and R. Gorden Jr., *J. Chem. Phys.*, **29**, 3341 (1963).
(28) V. Aquilanti, A. Galli, A. Giardini-Guidoni, and G. G. Volpi, *J. Chem. Phys.*, **48**, 4310 (1968).
(29) B. H. Solka, A. Y. K. Lam, and A. Harrison, *Can. J. Chem.*, **52**, 1798 (1974).

Ionic Solvation by Aprotic Solvents. Gas Phase Solvation of the Alkali Ions by Acetonitrile

W. R. Davidson and P. Kebarle*

Contribution from the Chemistry Department, University of Alberta, Edmonton, Alberta, Canada T6G 2E1.

Received February 25, 1976

Abstract: The ion equilibria in the gas phase ($M^+(CH_3CN)_{n-1}$ + CH_3CN = $M^+(CH_3CN)_n$) were measured for Na^+, K^+, Rb^+, and Cs^+ for n = 1 to 5. The measured temperature dependence of the equilibrium constants $K_{n-1,n}$ led to the evaluation of $\Delta H^\circ_{n-1,n}$, $\Delta G^\circ_{n-1,n}$, and $\Delta S^\circ_{n-1,n}$ for the above systems. Comparison with similar data for the halide negative ions and acetonitrile shows that the initial interactions (low n) are very much larger for positive ions than for negative ions. Electrostatic calculations for the complexes M^+CH_3CN, X^-CH_3CN, and M^+H_2O in which the charge distribution in the acetonitrile (and water) molecule is explicitly taken into account reproduce well the experimental $\Delta H_{0,1}$. These calculations show that the weak interaction of acetonitrile with negative ions is due to the diffuse distribution of the positive pole of the dipole over the C and H atoms of the molecule. On the other hand the concentrated negative charge on the accessible N atom leads to strong interactions with positive ions. The difference between positive and negative ion interactions with acetonitrile decreases as n is increased. At n = 5 the interactions with negative ions become slightly more favorable. Comparing the results for $M^+(CH_3CN)_n$ with those for $M^+(H_2O)_n$ one finds that for low n acetonitrile gives stronger binding. This is due to its higher dipole. However, as n increases the interactions with water become more favorable. The results can be used for an approximate prediction of the single ion free energies of solvation of the alkali and halide ions in acetonitrile. The present results agree best with the single ion energies of Case and Parsons. The measurements were performed with high pressure mass spectrometric apparatus.

Significant differences between the solvent effects of protic solvents (HOH, CH_3OH, etc.) and dipolar aprotic solvents like dimethylformamide, dimethyl sulfoxide, acetonitrile, and others have been observed in heterolic organic reactions.[1,2] These differences have been explained by the assumption that the solvation of negative ions by aprotic solvents is much weaker than that of positive ions of similar size and shape. Studies of the enthalpies of transfer[3] and activity coefficients[4] of alkali and halide ions in aprotic solvents have confirmed the weak solvation of negative ions. However, these investigations[3,4] were dependent on extra thermodynamic assumptions common to approaches in which properties of electrolytic so-